



## Study of the solvent effects on the formation of $\alpha$ -bromoglycidic esters in aliphatic series using the quantum DFT method with B3LYP/6-311G (d, p)

Z. Lakbaibi<sup>1</sup>, H. Abou El Makarim<sup>2</sup>, M. Tabyaoui<sup>3</sup>, A. El Hajbi<sup>4\*</sup>

<sup>1</sup>Chouaib Doukkali University, Faculty of Science, Department of Chemistry, Laboratory of Organic and Bioorganic Chemistry and Environment (LCOBE), BP20, 24000 El Jadida, Morocco

<sup>2</sup>Mohammed V University, Faculty of Science, Department of Chemistry, LS3ME Theoretical Chemistry and Molecular Modeling Team, BP1014 Avenue Ibn Batouta, Rabat, Morocco

<sup>3</sup>Mohammed V University, Faculty of Science, Department of Chemistry, Laboratory of Materials, Nanoparticles and Environment, BP 1014, Avenue Ibn Batouta, Rabat, Morocco

<sup>4</sup>Chouaib Doukkali University, Faculty of Science, Department of Chemistry, Laboratory of Physical Chemistry, BP20, 24000 El Jadida, Morocco

Received 01 Jul 2016, Revised 03 Nov 2016, Accepted 05 Nov 2016

\*For correspondence: Email: [a\\_elhajbi@yahoo.fr](mailto:a_elhajbi@yahoo.fr); Tel.: +212 (0)655759886

### Abstract

In the present work we used DFT B3LYP/6-311G (d, p) to study the effect of the solvent 2-propanol on the reaction between isopropyl dibromoacetate and isobutyraldehyde. We found that the energies of the reactants, the transition structures and the products of the reaction are all lower in the solvent than in the gas phase. We calculated the electrophilic and nucleophilic character of the reactants, the condensed local softness and certain thermodynamic quantities (enthalpy, entropy and Gibbs free energy). We used natural population analysis (NPA) to determine Fukui indices, electronic populations and reactivity indices. We found that all reactions were exothermic and that the process of formation of the new  $\sigma$  bonds ( $C_1-C_2$  and  $C_2-O_3$ ) was more synchronous in the gas phase than in the solvent. IRC calculations in both the gas phase and the solvent show that the transition structures are unique and occur early in the reaction.

**Keywords:** electronic atomic population, electrophilicity, Fukui index, nucleophilicity, reactivity index, transition state

### 1. Introduction

The application of the Darzens reaction to the synthesis of functional  $\alpha$ -halogenated epoxy compounds has been studied over many years from both the synthetic and mechanistic point of view [1].  $\alpha$ -brominated glycidic esters are prepared at ambient temperature using the Darzens reaction [1]. However, only the  $\alpha$ -brominated epoxy esters derived from aldehydes can be isolated; in all other cases isomerisation takes place immediately and leads to the formation of bromopyruvic esters. This reaction has been generalized to other  $\alpha$ -halogenated epoxy functional structures [2-3]. These glycidic esters and other  $\alpha$ -halogenated epoxy functional structures are easily opened by Lewis acids [2]. They are excellent synthesis intermediates which offer new ways of obtaining  $\alpha$ -functional derivatives of pyruvic acid [4] and acids, esters and amides [5] from a simple carbonyl derivative.

The  $\alpha$ -cetoesters themselves constitute an important intermediate in organic synthesis, particularly for the preparation of heterocycles [6-7]. This reaction occurs in two steps. The first step involves the aldol reaction of the enolates derived from dibromoacetate alkyl groups, these groups having previously been obtained by action of potassium alkoxide  $ROK^+$  in alcoholic solution with an aldehyde. The second step is an intramolecular nucleophilic substitution  $SN_i$  [1] in which the negatively charged oxygen attacks the carbon carrying the halogen, forming the epoxide [1].

Experimentally [1] it has been shown that the reaction between isobutyraldehyde and the isopropyl dibromoacetate in a protic solvent such as 2-propanol,  $\epsilon = 19.264$  leads to the formation of a glycidic ester which gives four diastereoisomers denoted  $P_1$  (1R, 2S),  $P_2$  (1S, 2R),  $P_3$  (1S, 2S) and  $P_4$  (1R, 2R) (Figure 1). The two cis diastereoisomers  $P_3$  (1S, 2S) and  $P_4$  (1R, 2R) are more stable than the trans isomers.

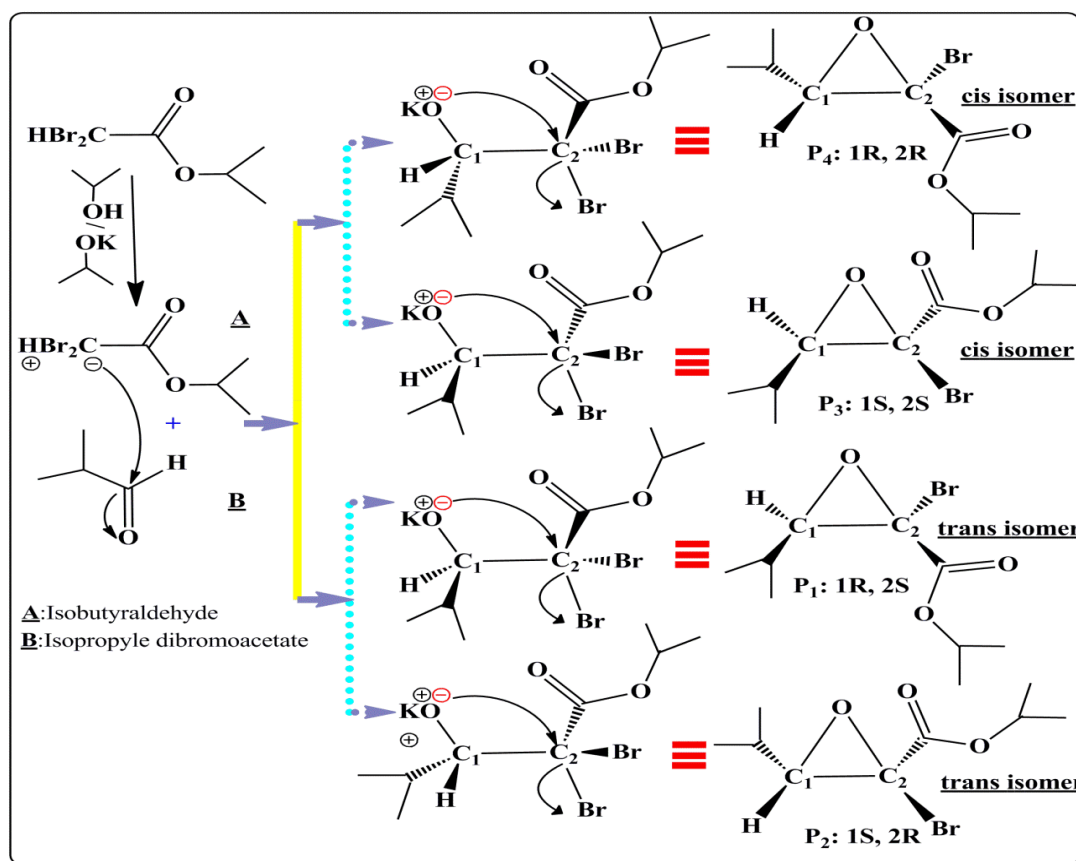


**Figure 1:** Reaction between isobutyraldehyde and isopropyl dibromoacetate

Our aim in this work was to gain greater understanding of the solvent effects on the reaction between isobutyraldehyde and isopropyl dibromoacetate when this takes place in the protic solvent 2-propanol. We used density functional theory (DFT) [8] as this method makes it possible to predict interatomic distances, total energies, relative energies and transition energies. The solvent effects were modeled using the polarizable continuum model (PCM) [9-11].

## 2. Chemical quantum calculation

All calculations were carried out with the program package Gaussian 09 [12] and displayed with GaussView [13]. We used the DFT computational method with the B3LYP hybrid functional, which includes the Becke gradient exchange correction and the Lee, Yang, and Parr correlation functional [14] combined with the 6-311(d, p) basis set [15]. The optimization thresholds were Max Force 0.000450, RMS Force 0.000300, Max Displacement 0.001800, and RMS Displacement 0.001200, all in atomic units. The optimization was stopped when all these conditions were satisfied. This particular set of values corresponds to the default convergence criteria in the Gaussian package. We began with the geometrical optimization of reactants, products and transition states. We then predicted the local responsiveness of reactants and the local electrophilicity and nucleophilicity indices. We analyzed the potential energy surface and the IRC (Intrinsic Reaction Coordinate) [16] and calculated enthalpy, entropy and Gibbs free energy, as well as the localization of transition states. Finally, the solvent effects were assessed using a relatively simple self-consistent reaction field (SCRf) [11, 17-19], based on the polarizable continuum model (PCM) of Tomasi's group [9-11]. We set the dielectric constant at 298.15 K,  $\epsilon = 19.264$  of 2-propanol.

## 3. Global and local reactivity descriptors derived from DFT

DFT [20] is a valuable source of chemical concepts as electronic chemical potential  $\mu$ , electronegativity  $\chi$ , hardness  $\eta$ , softness  $S$ , nucleophilicity  $N_u$ , electrophilicity  $\omega$ , global charge transfer  $\Delta N_{max}$  and reactivity descriptors such as Fukui indices  $f_k$ , local softness  $S_k$  and Parr function  $P(r)$ .

### 3.1 Global reactivity descriptors

Chemical potential  $\mu$  is defined by Parr et al [21] according to the following equation:

$$\mu = \left( \frac{\partial E}{\partial N} \right)_{v(r)} \quad (1)$$

where  $E$  is total energy,  $N$  is the number of electrons, and  $v(r)$  is the external potential of the system.

Domingo et al define hardness  $\eta$  as the second derivative of energy  $E$  [22]:

$$\eta = \left( \frac{\partial^2 E}{\partial N^2} \right)_{v(r)} \quad (2)$$

where  $N$  is number of electrons at constant external potential,  $v(r)$ .

Koopmans' theorem states that ionization potential  $I$  and electron affinity  $A$  can be expressed in terms of the energy of the highest occupied molecular orbital ( $\epsilon_{HOMO}$ ) and the lowest unoccupied molecular orbital ( $\epsilon_{LUMO}$ ) respectively [23]:

$$I \approx -\epsilon_{HOMO} \quad (3)$$

$$A \approx -\epsilon_{LUMO} \quad (4)$$

Once  $I$  and  $A$  are known, the following equations can be used to calculate absolute electronegativity  $\chi$ , hardness  $\eta$  and softness  $S$  [24]:

$$\chi \approx -\mu \approx \frac{1}{2}(I + A) \approx \frac{(-\epsilon_{HOMO} - \epsilon_{LUMO})}{2} \quad (5)$$

$$\eta \approx (I - A) \approx \epsilon_{LUMO} - \epsilon_{HOMO} \quad (6)$$

Softness  $S$  is the inverse of hardness  $\eta$  [25-27]:

$$S = \frac{1}{\eta} \quad (7)$$

When two systems with different electronegativities react together, electrons are transferred from the nucleophilic molecule to the electrophilic molecule until the chemical potentials are equal [28]. The number of electrons transferred  $\Delta N_{max}$  is calculated by the following expression [23]:

$$\Delta N_{max} = -\frac{\mu}{\eta} \quad (8)$$

Parr and al [23] have proposed a global electrophilicity index  $\omega$  as a measure of the reduction in energy due to the maximum electron transfer:

$$\omega = \frac{\mu^2}{2\eta} \quad (9)$$

High values of nucleophilicity correspond to low values of ionization potential and vice versa. Recently, Domingo et al. have introduced a relative nucleophilicity index  $N_u$  based on the HOMO energies obtained within the Kohn-Sham scheme [29] and defined as [22, 31]:

$$N_u = \epsilon_{HOMO(N_u)} - \epsilon_{HOMO(TCE)} \quad (10)$$

The nucleophilicity index  $N_u$  is referred to tetracyanoethylene (TCE) as this allows us to conveniently handle a nucleophilicity scale of positive values [22, 31].

### 3.2 Local reactivity descriptors

The Fukui functions corresponding to the site  $k$  of a molecule  $f_k$  are indicators that are used to identify the most favored nucleophile-electrophile attacks. The condensed form of the Fukui functions in a molecule with  $N$  electrons has been proposed by Yang and Mortar [24]:

- for a nucleophilic attack  $f_k^+ = [q_k(N + 1) - q_k(N)]$  (11)

- for an electrophilic attack  $f_k^- = [q_k(N) - q_k(N - 1)]$  (12)

where  $q_k(N)$ ,  $q_k(N-1)$  and  $q_k(N+1)$  are the populations of the electronic site  $k$  in the neutral system, cation and anion, respectively.

The condensed local softnesses  $S^\pm$  can be easily calculated from the condensed Fukui functions  $f_k^\pm$  and the global softness  $S$  [23]:

$$S^\pm = \left[ \frac{\partial \rho(r)}{\partial \mu} \right]_{v(r)} = \left[ \frac{\partial \rho(r)}{\partial N} \right] \left[ \frac{\partial N}{\partial \mu} \right]_{v(r)} = S f_k^\pm \quad (13)$$

Recently Domingo et al have proposed that Parr functions  $P(r)$  as given by the following equations can be used to predict local reactivity [30]:

- for an electrophilic attack  $P^-(r) = \rho_s^{rc}(r)$  (14)

- for a nucleophilic attack  $P^+(r) = \rho_s^{ra}(r)$  (15)

where  $\rho_s^{rc}(r)$  and  $\rho_s^{ra}(r)$  are the atomic spin densities (ASD) of the radical cation and anion respectively.

The local electrophilicity and local nucleophilicity indices of a site  $k$  in a molecule enable us to predict the most favored nucleophilic-electrophilic attack. These indices can be calculated using the Fukui functions [25-26] and the Parr functions [30] as follows:

$$\omega_k = \omega f_k^+ \quad (16)$$

$$Nu_k = Nu f_k^- \quad (17)$$

$$\omega_k = \omega P_k^+ \quad (18)$$

$$Nu_k = Nu P_k^- \quad (19)$$

The maximum charge transfer can be written as follows [23]:

$$\Delta N_{max} = \sum_k \Delta N_{max}(k) = -\sum_k S_k^+ = -\sum_k S_k^- = -\sum_k f_k^+ = \Delta N_{max} \sum_k f_k^+ \quad (20)$$

This gives an additional expression for the regional maximum transfer charge that an atom  $k$  in the electrophile can acquire from its environment. This expression is as follows [22]:

$$\Delta N_{max}(k) = \Delta N_{max} f_k^+ \quad (21)$$

## 4. Results and discussion

### 4.1 Geometry optimization and charge density calculation of the reactants in the gas phase and in 2-propanol solution

We used DFT B3LYP/ 6-311G (d, p) to calculate the atomic charge densities and interatomic distances of the reactants isobutyraldehyde and isopropyl dibromoacetate. Table 1 shows the charge densities while Table 2 shows the interatomic distances. Optimized geometries of the two reactants in the gas phase and in 2-propanol are given in Figures 2 and 3, and isodensity maps of the HOMO and LUMO orbitals are shown in Figures 4 and 5.

**Table 1:** Atomic charge densities of isobutyraldehyde and isopropyl dibromoacetate in the gas phase and in 2-propanol solution (Coulomb)

Isobutyraldehyde			Isopropyl dibromoacetate		
Atoms	Gas phase	2-propanol solution	Atoms	Gas phase	2-propanol solution
C <sub>(1)</sub>	+0.197	+0.215	C <sub>(14)</sub>	-0.605	-0.566
O <sub>(2)</sub>	-0.276	-0.328	O <sub>(2)</sub>	-0.366	-0.456
H <sub>(3)</sub>	+ 0.070	+0.081	O <sub>(3)</sub>	-0.446	-0.370
C <sub>(4)</sub>	-0.259	-0.241	C <sub>(4)</sub>	+0.003	-0.004
H <sub>(5)</sub>	+0.131	+0.130	C <sub>(5)</sub>	-0.261	-0.278
C <sub>(6)</sub>	-0.258	-0.292	C <sub>(6)</sub>	-0.284	-0.279
C <sub>(10)</sub>	-0.289	-0.292	C <sub>(1)</sub>	+0.485	+0.473
H <sub>(7)</sub>	+0.119	+0.122	H <sub>(7)</sub>	+0.143	+0.123
H <sub>(8)</sub>	+0.104	+0.117	H <sub>(10)</sub>	+0.131	+0.114
H <sub>(9)</sub>	+0.112	+0.124	H <sub>(8)</sub>	+0.108	+0.110
H <sub>(11)</sub>	+0.119	+0.124	H <sub>(9)</sub>	+0.084	+0.107
H <sub>(12)</sub>	+0.111	+0.117	H <sub>(11)</sub>	+0.139	+0.113
H <sub>(13)</sub>	+0.117	+0.122	H <sub>(12)</sub>	+0.110	+0.109
			H <sub>(13)</sub>	+0.069	+0.112
			Br <sub>(15)</sub>	-0.023	-0.119
			Br <sub>(16)</sub>	-0.087	-0.119
			K <sub>(17)</sub>	+0.802	+0.930

In isopropyl dibromoacetate the atom with the highest charge density, in both gas phase and in solution, is C<sub>(14)</sub>; in isobutyraldehyde it is C<sub>(1)</sub>, indicating that C<sub>(1)</sub> and C<sub>(14)</sub> are the likely sites of attack in this reaction.

Table 2 shows that in isobutyraldehyde in 2-propanol solution interatomic distances are equal for several pairs of bonds, namely C<sub>10</sub>-O<sub>2</sub> and C<sub>6</sub>-O<sub>2</sub>; C<sub>6</sub>-C<sub>1</sub> and C<sub>10</sub>-C<sub>1</sub>; C<sub>6</sub>-C<sub>4</sub> and C<sub>10</sub>-C<sub>4</sub>; C<sub>6</sub>-H<sub>3</sub> and C<sub>10</sub>-H<sub>3</sub>; and C<sub>10</sub>-H<sub>5</sub> and C<sub>6</sub>-H<sub>5</sub>. Similarly, atoms C<sub>(10)</sub> and C<sub>(6)</sub> have the same charge density (Table 1). This suggests that interatomic distances as well as charge density in this reactant are influenced by the solvent effect. In isopropyl dibromoacetate it is the bromine atoms Br<sub>(15)</sub> and Br<sub>(16)</sub> which have the same charge density in 2-propanol solution. However the interatomic distance C<sub>(14)</sub>-Br<sub>(16)</sub> (1.976 Å) is higher than that of C<sub>(14)</sub>-Br<sub>(15)</sub> (1.584 Å). This leads us to conclude that the atom Br<sub>(16)</sub> is easily detached.

**Table 2:** Interatomic distances in isobutyraldehyde and isopropyl dibromoacetate in the gas phase and in 2-propanol solvent (Å)

Isobutyraldehyde			Isopropyl dibromoacetate		
Interatomic distances	Gas phase	2-propanol solution	Interatomic distances	Gas phase	2-propanol solution
C <sub>1</sub> -O <sub>2</sub>	1.204	1.209	C <sub>1</sub> -O <sub>2</sub>	1.214	1.229
C <sub>1</sub> -C <sub>4</sub>	1.517	1.511	C <sub>1</sub> -O <sub>3</sub>	1.423	1.371
H <sub>7</sub> -C <sub>4</sub>	2.174	2.190	C <sub>4</sub> -O <sub>3</sub>	1.451	1.454
C <sub>1</sub> -H <sub>3</sub>	1.115	1.113	C <sub>4</sub> -H <sub>7</sub>	1.091	1.092
C <sub>4</sub> -C <sub>6</sub>	1.528	1.539	C <sub>1</sub> -C <sub>14</sub>	1.439	1.445
C <sub>4</sub> -C <sub>10</sub>	1.541	1.539	C <sub>4</sub> -C <sub>5</sub>	1.522	1.525
C <sub>6</sub> -C <sub>1</sub>	2.529	2.490	C <sub>4</sub> -C <sub>6</sub>	1.526	1.522
C <sub>10</sub> -C <sub>1</sub>	2.497	2.490	K <sub>17</sub> -Br <sub>15</sub>	4.406	3.781
C <sub>6</sub> -O <sub>2</sub>	2.827	3.445	K <sub>17</sub> -Br <sub>16</sub>	3.152	3.796
C <sub>10</sub> -O <sub>2</sub>	3.497	3.445	O <sub>3</sub> -H <sub>7</sub>	2.058	2.067
C <sub>6</sub> -H <sub>3</sub>	3.526	2.808	O <sub>2</sub> -H <sub>7</sub>	2.327	2.344
C <sub>10</sub> -H <sub>3</sub>	2.747	2.808	C <sub>6</sub> -H <sub>11</sub>	1.091	1.092
C <sub>6</sub> -H <sub>5</sub>	2.161	2.169	C <sub>6</sub> -H <sub>12</sub>	1.097	1.094
C <sub>10</sub> -H <sub>5</sub>	2.142	2.169	C <sub>6</sub> -H <sub>13</sub>	1.094	1.093
H <sub>5</sub> -O <sub>2</sub>	3.053	2.529	C <sub>14</sub> -Br <sub>15</sub>	1.933	1.584
H <sub>5</sub> -H <sub>3</sub>	2.497	3.080	C <sub>14</sub> -Br <sub>16</sub>	2.007	1.976
C <sub>6</sub> -H <sub>7</sub>	1.091	1.093	C <sub>14</sub> -K <sub>17</sub>	2.738	2.891
C <sub>6</sub> -H <sub>8</sub>	1.093	1.094	Br <sub>15</sub> -O <sub>2</sub>	3.132	4.081
C <sub>6</sub> -H <sub>9</sub>	1.093	1.093	Br <sub>16</sub> -O <sub>2</sub>	4.040	3.096
C <sub>10</sub> -H <sub>11</sub>	1.092	1.093	K <sub>17</sub> -O <sub>2</sub>	4.108	4.363
C <sub>10</sub> -H <sub>12</sub>	1.094	1.094	Br <sub>15</sub> -O <sub>3</sub>	4.128	3.006
C <sub>10</sub> -H <sub>13</sub>	1.094	1.093	Br <sub>16</sub> -O <sub>3</sub>	3.064	4.084
H <sub>7</sub> -O <sub>2</sub>	2.736	3.436	K <sub>17</sub> -O <sub>3</sub>	2.679	4.292
H <sub>8</sub> -O <sub>2</sub>	3.905	3.843	C <sub>5</sub> -H <sub>8</sub>	1.091	1.091
H <sub>9</sub> -O <sub>2</sub>	2.860	4.368	C <sub>5</sub> -H <sub>9</sub>	1.093	1.093
H <sub>11</sub> -O <sub>2</sub>	4.429	4.368	C <sub>5</sub> -H <sub>10</sub>	1.095	1.094
H <sub>12</sub> -O <sub>2</sub>	3.834	3.842	H <sub>8</sub> -O <sub>2</sub>	4.271	2.777
H <sub>13</sub> -O <sub>2</sub>	3.557	3.436	H <sub>9</sub> -O <sub>2</sub>	4.728	4.023
H <sub>7</sub> -H <sub>3</sub>	3.807	3.170	H <sub>10</sub> -O <sub>2</sub>	4.706	3.961
H <sub>8</sub> -H <sub>3</sub>	4.364	2.608	H <sub>11</sub> -O <sub>2</sub>	2.701	4.252
H <sub>9</sub> -H <sub>3</sub>	3.849	3.807	H <sub>12</sub> -O <sub>2</sub>	3.945	4.685
H <sub>11</sub> -H <sub>3</sub>	3.739	3.807	H <sub>13</sub> -O <sub>2</sub>	3.961	4.739
H <sub>12</sub> -H <sub>3</sub>	2.494	2.608			
H <sub>13</sub> -H <sub>3</sub>	3.145	3.171			

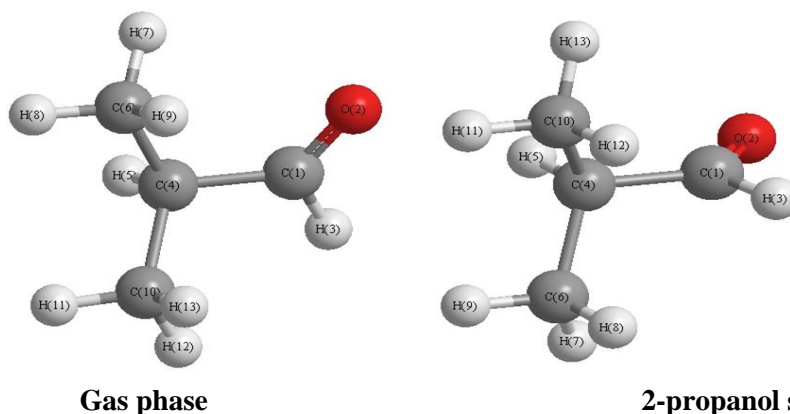


**Figure 2:** Optimized structure of isobutyraldehyde in the gas phase and in 2-propanol solvent

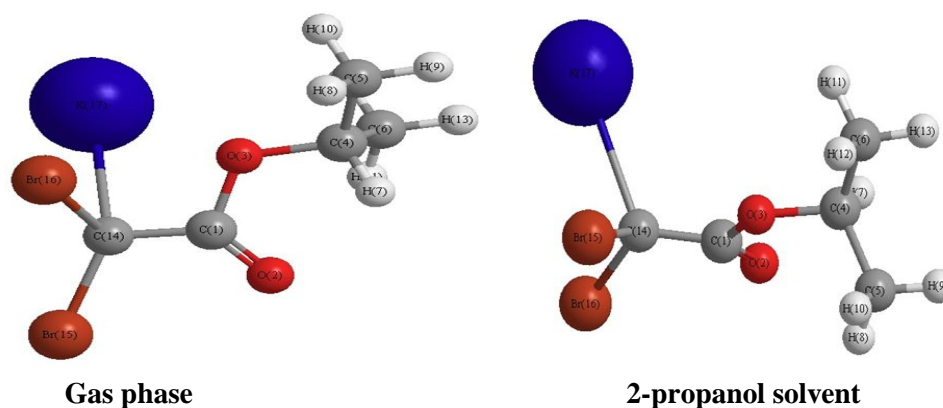


**Figure 3:** Optimized structure of isopropyl dibromoacetate in the gas phase and in 2-propanol solvent

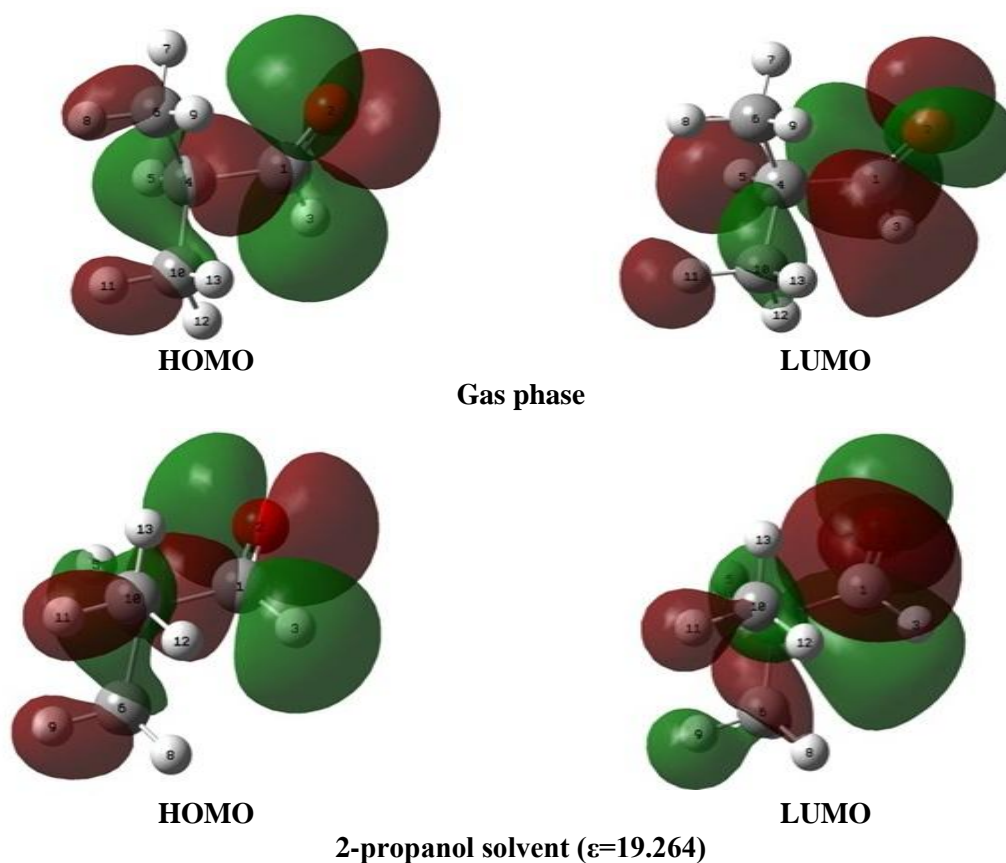


**Figure 4:** HOMO and LUMO isodensity maps of isobutyraldehyde in the gas phase and in 2-propanol solvent

Isodensity maps show that in isopropyl dibromoacetate the HOMO is very much localized on the carbon atom  $C_{(14)}$ , in both gas phase and solvent, whereas in isobutyraldehyde the LUMO is concentrated on  $C_{(1)}$ . We therefore conclude that the attack takes place preferentially between  $C_{(14)}$  of isopropyl dibromoacetate and  $C_{(1)}$  of isobutyraldehyde.

We also found that while the 2-propanol solvent effect did not substantially modify the geometry of isobutyraldehyde, it did have an effect on the structure of isopropyl dibromoacetate.

#### 4.2 Predicting the normal electron demand and inverse electron demand in the gas phase and in 2-propanol solution

We calculated the electronic chemical potential  $\mu$ , electrophilicity index  $\omega$ , hardness  $\eta$  and nucleophilicity index  $Nu$  of both reactants in the gas phase and in 2-propanol solution. We also calculated global and local indices of reactivity, as these provide effective tools for studying the reactivity of polar interactions [32]. We calculated

HOMO and LUMO energies, maximum global charge transfer  $\Delta N_{max}$ , and finally we determined the difference in electrophilicity between the two reactants  $\Delta\omega$  (Table 3). These chemical properties enabled us to determine the relative electrophilic or nucleophilic character of isobutyraldehyde and isopropyl dibromoacetate.

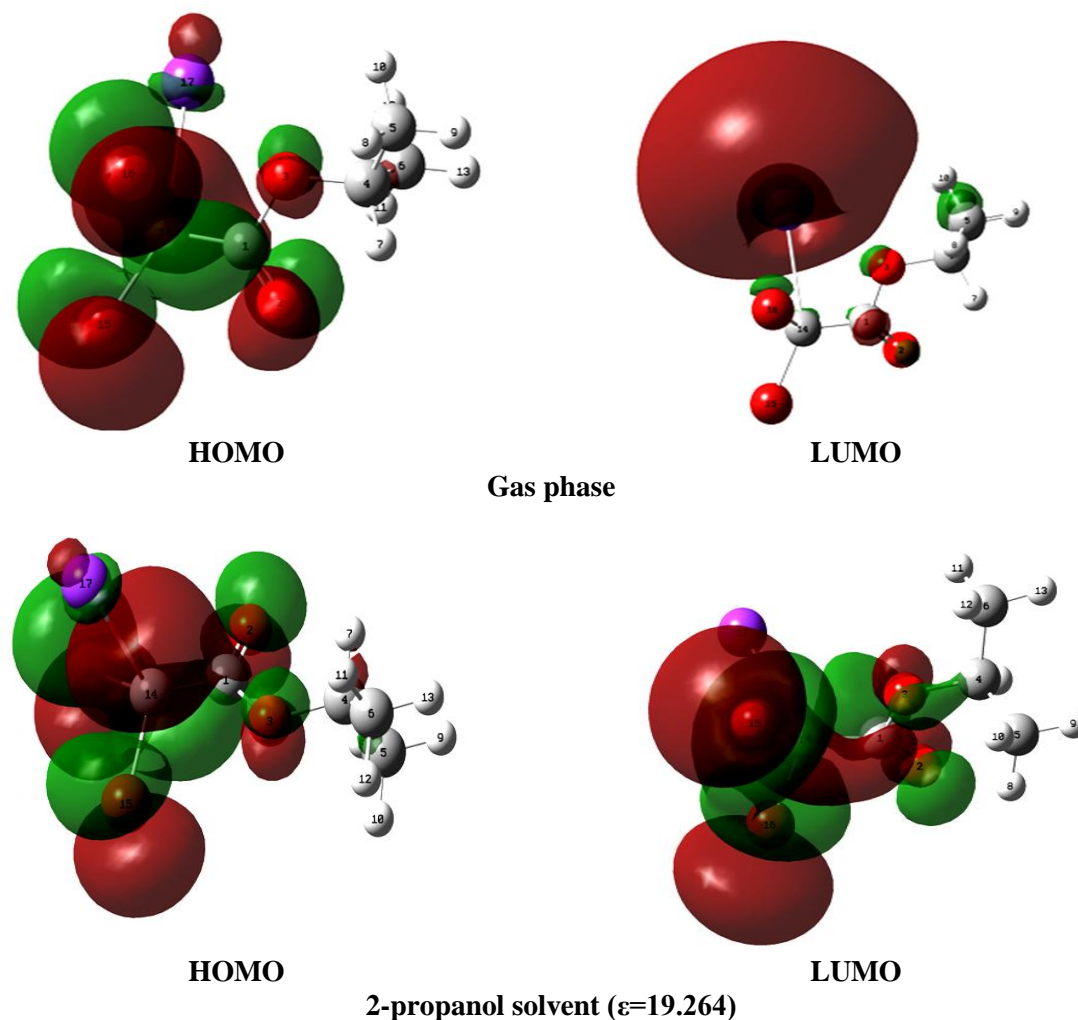


**Figure 5:** HOMO and LUMO isodensity maps of isopropyl dibromoacetate in the gas phase and in 2-propanol solvent

Isodensity maps of the HOMO/LUMO energies of isobutyraldehyde and isopropyl dibromoacetate in the gas phase and in solution are given in Figures 4 and 5 respectively.

Notes to Table 3:

- $e$  = elementary charge  $1.6 \cdot 10^{-19}$  C
- $\Delta\omega = |\omega \text{ isopropyl dibromoacetate} - \omega \text{ isobutyraldehyde}|$
- $E_{HOMO} \text{ TCE}^{(a)} = -9.369$  eV calculated by DFT (B3LYP)/6-311G (d, p) in the gas phase
- $E_{HOMO} \text{ TCE}^{(a)} = -8.997$  eV calculated by DFT (B3LYP)/6-311G (d, p) in 2-propanol solvent

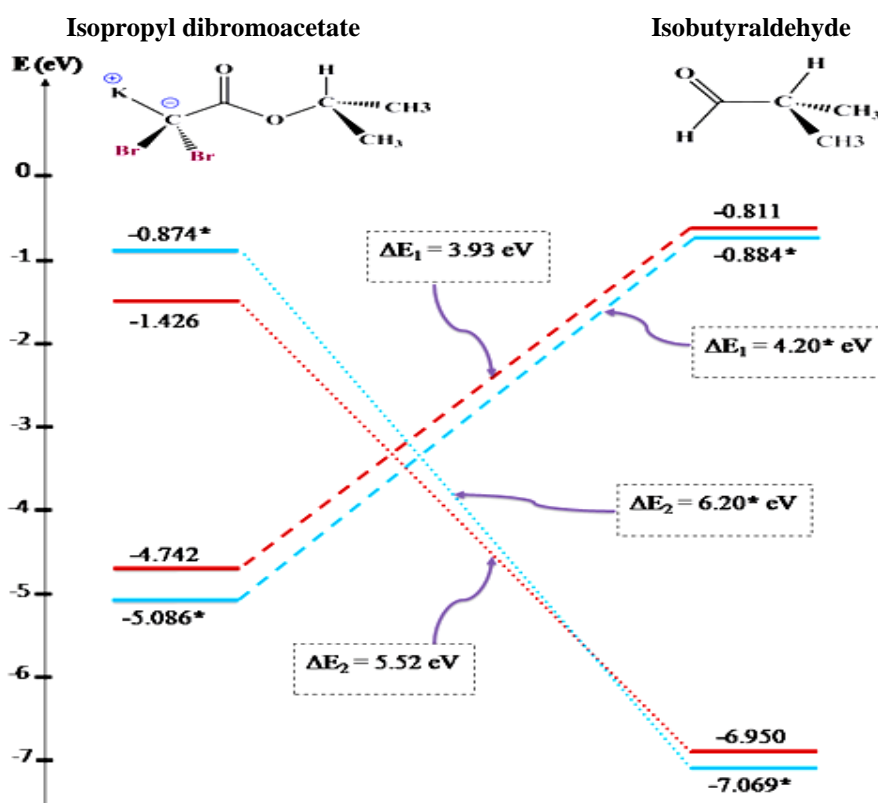
A comprehensive study carried out in 2002 by Domingo et al. on the electrophilicity of a number of reactants involved in Diels-Alder reactions provided a single electrophilicity  $\omega$  scale in which tetracyanoethylene (TCE;  $\omega = 5.96$  eV) as the most highly electrophilic is used as a reference [22]. TCE is also a convenient reference for studying isobutyraldehyde and isopropyl dibromoacetate (Table 3).

Table 3 shows that the electronic chemical potential  $\mu$  of isopropyl dibromoacetate is higher than that of isobutyraldehyde, while the global nucleophilicity index  $Nu$  of isobutyraldehyde is lower than that of isopropyl dibromoacetate. This implies that electrons are transferred from isopropyl dibromoacetate to isobutyraldehyde.

**Table 3:** HOMO and LUMO energies (eV), electronic chemical potential  $\mu$  (eV), global hardness  $\eta$  (eV), global softness  $S$  (eV<sup>-1</sup>), electrophilicity index  $\omega$  (eV), nucleophilicity index  $Nu$  (eV), maximum charge transfer  $\Delta N_{max}$ , and difference  $\Delta\omega$  (eV) in the gas phase and in 2-propanol solution

	Isobutyraldehyde		Isopropyl dibromoacetate		
	Gas phase	2-propanol solution	Gas phase	2-propanol solution	
$E_{HOMO}$	-6.950	-7.069	$E_{HOMO}$	-4.742	-5.086
$E_{LUMO}$	-0.811	-0.883	$E_{LUMO}$	-1.426	-0.873
$\mu$	-3.880	-3.679	$\mu$	-3.084	-2.980
$\eta$	6.139	6.185	$\eta$	3.315	4.213
$S$	0.163	0.162	$S$	0.302	0.237
$\omega$	1.226	1.278	$\omega$	1.434	1.054
$Nu$	2.418	1.928	$Nu$	4.627	3.911
$\Delta N_{max}$	0.632 e	0.643 e	$\Delta N_{max}$	0.930 e	0.707 e
$\Delta\omega$	Gas phase		$\Delta\omega$	2-propanol solution	
	0.21			0.22	

The hardness of the isopropyl dibromoacetate is lower than that of isobutyraldehyde which means that electron transfer takes place from the isopropyl dibromoacetate to the isobutyraldehyde in both the gas phase and in the solvated phase. Moreover, as the overall hardness of the two reactants increases under the effect of the solvent, their molecular structure changes from a relatively less stable form in the gas phase to a more stable form in 2-propanol solution [33-36].



**Figure 6:** Correlation diagram between the HOMO and LUMO of isobutyraldehyde and isopropyl dibromoacetate in the gas phase and in 2-propanol solution  
 \* Values followed by an asterisk refer to 2-propanol solution.

Table 3 shows that the global electrophilicity  $\omega$  and global maximum electron transfer  $\Delta N_{max}$  of the electrophilic compound (isobutyraldehyde) is increased by the 2-propanol solvent. The global nucleophilicity  $Nu$  and global maximum electron transfer  $\Delta N_{max}$  of the nucleophilic compound (isopropyl dibromoacetate) is reduced by the

solvent. The low value of the global maximum electron transfer  $\Delta N_{max}$  between isopropyl dibromoacetate and isobutyraldehyde, as well as the relatively small difference in electrophilicity  $\Delta\omega$  between isopropyl dibromoacetate and isobutyraldehyde, in both gas phase and solution, indicates that this reaction is weakly polar in character. Global electrophilicity  $\omega$  of isobutyraldehyde in both the gas phase and in 2-propanol solution is moderate, showing that the 2-propanol solvent does not significantly alter the global electrophilicity of this reactant [22]. Global nucleophilicity  $Nu$  of isopropyl dibromoacetate is relatively strong in both gas phase and 2-propanol solvent, and is not significantly altered by the solvent effect [33, 37].

The correlation diagram (Figure 6) shows that the energy gaps  $\Delta E_1$  and  $\Delta E_2$  are respectively 3.93 eV (gas phase), 4.20 eV (solution) and 5.50 eV (gas phase), 6.20 eV (solution). The interaction takes place between the HOMO of one reactant and the LUMO of the other, with the interaction with the lowest energy difference between the two being preferred [38]. Thus the most favorable interaction is between the HOMO of isopropyl dibromoacetate and the LUMO of isobutyraldehyde, which is a normal electronic demand (NED) reaction [39].

#### 4.3 Predicting local reactivity in the gas phase and in 2-propanol solution

##### 4.3.1 Chattaraj's polar model

According to Chattaraj's polar model [40-41], the local electrophilicity and nucleophilicity indices  $\omega_k$  and  $Nu_k$  can reliably predict the most favored electrophilic-nucleophilic interaction between two polar centers. The most favored regioisomer is the one with the highest local electrophilicity index  $\omega_k$  and the highest local nucleophilicity index  $Nu_k$ . Following on from the work of Chattaraj and Domingo [25] we propose a new descriptor,  $\Delta Z$ , corresponding to the difference between the highest value of local nucleophilicity  $Nu_k$  and the highest value of local electrophilicity  $\omega_k$  of the reactant. The more closely  $\Delta Z$  approaches to zero, the more the interaction is favored. The  $\omega_k$  values of the atoms in isobutyraldehyde and the  $Nu_k$  values of the atoms in isopropyl dibromoacetate as well as the global maximum electron transfer  $\Delta N_{max}(k)$  of isobutyraldehyde and  $\Delta Z$  are reported in Table 4. These results allow us to predict the electrophilic and nucleophilic interactions, the reaction path and the chemoselectivity.

**Table 4:** Electronic populations, Fukui functions, local electrophilicity  $\omega_k$  of isobutyraldehyde, local nucleophilicity  $Nu_k$  of isopropyl dibromoacetate, local maximum electron transfer  $\Delta N_{max}(k)$  (e) for isobutyraldehyde and the difference  $\Delta Z$  (eV) in the gas phase and in 2-propanol solution

Isobutyraldehyde		C <sub>(1)</sub>	O <sub>(2)</sub>	C <sub>(4)</sub>	C <sub>(10)</sub>	C <sub>(6)</sub>	H <sub>(3)</sub>	H <sub>(5)</sub>
Electronic population	$q_k(N)$	5.550 5.531*	8.520 8.561*	6.297 6.290*	6.578 6.572*	6.581 6.572*	0.895 0.895*	0.786 0.792*
	$q_k(N+I)$	5.971 5.998*	8.750 8.808*	6.273 6.262*	6.580 6.576*	6.576 6.576*	0.962 0.976*	0.827 0.830*
Local indices	$f_k^+$	0.421 0.467*	0.230 0.247*	-0.024 -0.028*	0.002 0.004*	-0.005 0.004*	0.067 0.081*	0.041 0.038*
	$\omega_k$ (eV)	0.516 0.597*	0.282 0.316*	-0.029 -0.036*	0.002 0.005*	0.006 0.005*	0.082 0.101*	0.050 0.048*
	$\Delta N_{max}(k)$	0.266 0.300*	0.145 0.159*	-0.015 -0.018*	0.001 0.003*	0.003 0.003*	0.042 0.053*	0.026 0.024*
Isopropyl dibromoacetate		C <sub>(1)</sub>	O <sub>(2)</sub>	O <sub>(3)</sub>	C <sub>(14)</sub>	Br <sub>(15)</sub>	Br <sub>(16)</sub>	K <sub>(17)</sub>
Electronic population	$q_k(N)$	5.211 5.313*	8.648 8.704*	8.569 8.601*	6.817 6.604*	35.013 35.056*	35.008 35.050*	18.071 18.026*
	$q_k(N-I)$	5.263 5.316*	8.585 8.571*	8.546 8.557*	6.451 6.288*	34.766 34.828*	34.766 34.825*	18.027 18.017*
Local indices	$f_k^-$	-0.052 -0.003*	0.063 0.133*	0.023 0.044*	0.366 0.316*	0.246 0.228*	0.242 0.225*	0.044 0.009*
	$Nu_k$ (eV)	-0.241 -0.012*	0.291 0.520*	0.106 0.172*	1.693 1.236*	1.138 0.892*	1.120 0.880*	0.203 0.035*
$\Delta Z$ (eV)		1.18 0.64*						

\* in 2-propanol solution

Notes to Table 4:

- $q_k(N)$ ,  $q_k(N - 1)$ , and  $q_k(N + 1)$  are the electronic populations of site  $k$  in the neutral system, the cation and the anion respectively.
- $\Delta Z = |Nu(C_{(14)}) - \omega(C_{(1)})|$  is the difference between the highest value of  $Nu_k$  in the nucleophilic reactant and the highest value of  $\omega_k$  in the electrophilic reactant.

Firstly, they show that the most favored interaction takes place between the  $C_{(14)}$  atom of the isopropyl dibromoacetate (highest value of  $Nu_k$ ) and the  $C_{(1)}$  atom of isobutyraldehyde (highest value of  $\omega_k$ ) in both the presence and the absence of 2-propanol solution. In other words, Chattaraj's polar model correctly predicts the formation of the  $C_{(14)}-C_{(1)}$  bond which is observed experimentally [1].

Secondly, the  $C_{(1)}$  atom of isobutyraldehyde has a higher local maximum electron transfer ( $\Delta N_{\max}(C_{(1)})=0.266$  e,  $0.300$  e\*) than the other atoms. This confirms that electron transfer takes place preferentially from the  $C_{(14)}$  atom of isopropyl dibromoacetate to the  $C_{(1)}$  atom of isobutyraldehyde.

Thirdly, Table 4 shows that both the local electrophilicity of the  $C_{(1)}$  atom and the local maximum electron transfer ( $\Delta N_{\max}(C_{(1)})$ ) of isobutyraldehyde are higher in solution than in the gas phase, increasing from  $0.516$  eV to  $0.597$  eV\* and from  $0.266$  e to  $0.300$  e\*, respectively. In contrast, the local nucleophilicity of the  $C_{(14)}$  atom in isopropyl dibromoacetate decreases from  $1.693$  eV to  $1.236$  eV\* as a result of the solvent effect.

The  $\Delta Z$  value in 2-propanol solution ( $\Delta Z = 0.64$  eV\*) is smaller than that in the gas phase ( $\Delta Z = 1.18$  eV), indicating that the  $C_{(1)}-C_{(14)}$  attack is more favored in solution than in the gas phase.

#### 4.3.2 Gazquez-Mendez rules

The Gazquez-Mendez rules state that the interaction between two chemical species A and B is favored when it occurs between atoms whose softnesses are approximately equal [42].

We used natural population analysis (NPA) to calculate the local softness  $S_k^+$  and  $S_k^-$  of the atoms of isobutyraldehyde and isopropyl dibromoacetate respectively [43]. Results are summarized in Table 5.

**Table 5:** Local softness ( $S_k^+$  and  $S_k^-$ ) of isobutyraldehyde and isopropyl dibromoacetate atoms in the gas phase and in 2-propanol solution, calculated using natural population analysis (NPA)

<b>Isobutyraldehyde</b>	<b>C<sub>(1)</sub></b>	<b>O<sub>(2)</sub></b>	<b>C<sub>(4)</sub></b>	<b>C<sub>(10)</sub></b>	<b>C<sub>(6)</sub></b>	<b>H<sub>(3)</sub></b>	<b>H<sub>(5)</sub></b>
<b>Local softness <math>S_k^+</math></b>	0.069 0.076*	0.038 0.044*	-0.004 -0.005*	0.001 0.002*	-0.001 0.001*	0.011 0.013*	0.007 0.006*
<b>Isopropyl dibromoacetate</b>	<b>C<sub>(1)</sub></b>	<b>O<sub>(2)</sub></b>	<b>O<sub>(3)</sub></b>	<b>C<sub>(14)</sub></b>	<b>Br<sub>(15)</sub></b>	<b>Br<sub>(16)</sub></b>	<b>K<sub>(17)</sub></b>
<b>Local softness <math>S_k^-</math></b>	-0.016 -0.001*	0.019 0.032*	0.006 0.010*	0.110 0.074*	0.074 0.054*	0.073 0.053*	0.013 0.002*

\* in 2-propanol solution

The local softness calculated in the gas phase and in solution show that the most favoured interaction is of the soft-soft type [42], and takes place between the  $C_{(1)}$  atom of isobutyraldehyde (highest value of  $S_k^+$ ) and the  $C_{(14)}$  atom of isopropyl dibromoacetate (highest value of  $S_k^-$ ). It follows that the soft-soft interaction is more highly favored in 2-propanol solution (where local softnesses are approximately equal) than in the gas phase (where local softnesses are not approximately equal).

We can therefore conclude that the formation of the  $C_{(14)}-C_{(1)}$  bond which is experimentally observed [1] in 2-propanol solution is correctly predicted by the Gazquez-Mendez rule.

#### 4.3.3 Theoretical study of frontier molecular orbitals (FMO)

According to Houk's rule [43], in a pericyclic process (reaction with four centers) large-large and small-small interactions are favored relative to large-small and small-large interactions, while in a non-pericyclic process (reaction with two centers) the first link is formed by a large-large interaction.

The atomic coefficients of the HOMO [44] of isopropyl dibromoacetate and the LUMO of isobutyraldehyde in the absence and presence of 2-propanol solution are given in Table 6.

Table 6 shows that the coefficient of  $C_{(1)}$  in the LUMO of isobutyraldehyde is greater than that of the other atoms and also that  $C_{(14)}$  has the highest coefficient in the HOMO of isopropyl dibromoacetate. This indicates that the

most favorable interaction is large-large, and takes place between the atomic orbital of the C<sub>(14)</sub> atom of isopropyl dibromoacetate and the atomic orbital of the C<sub>(1)</sub> atom of isobutyraldehyde. These results confirm yet again that (C<sub>(14)</sub>-C<sub>(1)</sub>) bonding is the most favored.

**Table 6:** Atomic coefficients of the HOMO of the isopropyl dibromoacetate R<sub>2</sub> and the LUMO of the isobutyraldehyde in the gas phase and in 2-propanol solution

<b>Isobutyraldehyde</b>		<b>C<sub>(1)</sub></b>	<b>O<sub>(2)</sub></b>	<b>C<sub>(4)</sub></b>	<b>H<sub>(3)</sub></b>
	LUMO coefficient	0.631 0.656*	-0.428 -0.429*	-0.472 -0.523*	-1.061 -1.100*
<b>Isopropyl dibromoacetate</b>		<b>C<sub>(1)</sub></b>	<b>O<sub>(2)</sub></b>	<b>O<sub>(3)</sub></b>	<b>C<sub>(14)</sub></b>
	HOMO coefficient	-0.155 -0.155*	0.291 0.296*	-0.156 0.174*	0.298 0.305*

\* in 2-propanol solution

#### 4.3.4 Calculation of local electrophilicity $\omega_k$ and local nucleophilicity $Nu_k$ using the electrophilic and nucleophilic Parr functions $P_k^+$ and $P_k^-$

We used the electrophilic Parr functions  $P_k^+$  to calculate the local electrophilicity  $\omega_k$  of the cationic molecule (isobutyraldehyde), and the nucleophilic Parr functions  $P_k^-$  to calculate the local nucleophilicity  $Nu_k$  of the anionic molecule (isopropyl dibromoacetate). We also calculated the difference  $\Delta Z$  between the highest value of  $Nu_k$  in isobutyraldehyde and the highest value of  $\omega_k$  in isopropyl dibromoacetate.

The Parr functions  $P_k^+$  and  $P_k^-$  were obtained by Mulliken analysis of the atomic spin density (ASD) of the cationic and anionic molecule respectively. The values of  $P_k^+$ ,  $P_k^-$  and the  $\Delta Z$  descriptor are given in Table 7.

**Table 7:** Parr functions  $P_k^+$  and  $P_k^-$ , local electrophilicity  $\omega_k$  of the cationic atoms in isobutyraldehyde (R<sub>1</sub>) and local nucleophilicity  $Nu_k$  for the anionic atoms in isopropyl dibromoacetate (R<sub>2</sub>) and the difference  $\Delta Z$  in the gas phase and in 2-propanol solvent

<b>R<sub>1</sub></b>	<b>Atom</b>		<b>C<sub>(1)</sub></b>	<b>O<sub>(2)</sub></b>	<b>C<sub>(4)</sub></b>	<b>C<sub>(10)</sub></b>	<b>C<sub>(6)</sub></b>	<b>H<sub>(3)</sub></b>	<b>H<sub>(5)</sub></b>
	<b>Local index</b>	$P_k^+$	0.568 0.655*	0.327 0.317*	-0.059 -0.078*	-0.004 0.017*	0.011 0.017*	-0.039 -0.043*	0.004 -0.001*
		$\omega_k$ (eV)	0.697 0.836*	0.400 0.405*	-0.071 -0.092*	-0.005 0.022*	0.013 0.022*	-0.048 -0.055*	0.005 -0.001*
	<b>Atom</b>		<b>C<sub>(1)</sub></b>	<b>O<sub>(2)</sub></b>	<b>O<sub>(3)</sub></b>	<b>C<sub>(14)</sub></b>	<b>Br<sub>(15)</sub></b>	<b>Br<sub>(16)</sub></b>	<b>K<sub>(17)</sub></b>
<b>R<sub>2</sub></b>	<b>Local index</b>	$P_k^-$	-0.005 -0.040*	-0.003 0.112*	0.013 0.021*	0.638 0.660*	0.168 0.119*	0.165 0.119*	0.015 0.006*
		$Nu_k$ (eV)	-0.025 -0.157*	-0.012 0.437*	0.060 0.082*	2.953 2.580*	0.778 0.467*	0.761 0.463*	0.071 0.022*
	$\Delta Z$ (eV)		2.26 1.74*						

\* in 2-propanol solution

The results in Table 7 show that the most favored interaction is between the C<sub>(14)</sub> atom of isopropyl dibromoacetate ( $Nu_{C_{(14)}}=2.953$  eV, 2,580 eV\*) and the C<sub>(1)</sub> atom of isobutyraldehyde ( $\omega_{C_{(1)}}=0.697$  eV, 0.836 eV\*).  $\Delta Z$  is lower in the 2-propanol solvent (1.74 eV) than in the gas phase (2.23 eV), indicating that the C<sub>(14)</sub>-C<sub>(1)</sub> attack is promoted by the solvation effect.

This result shows that the C<sub>(14)</sub>-C<sub>(1)</sub> attack is not correctly predicted by the Parr functions [30]; however this attack is predicted by the Fukui functions [25-26].

#### 4.4 Reaction mechanism

##### 4.4.1 Thermodynamic study

Table 8 brings together a number of thermodynamic quantities characterizing the condensation reaction of isobutyraldehyde with isopropyl dibromoacetate in the gas phase and in solution.

**Table 8:** Thermodynamic quantities characterizing the condensation reaction between isopropyl dibromoacetate and isobutyraldehyde in the gas phase and in 2-propanol solution calculated by DFT B3LYP/6-311G (d, p)

	Path (1R, 2S)	Path (1S, 2R)	Path (1S, 2S)	Path (1R, 2R)
$\Delta H$ (kcal/mol)	-20.535 -34.984*	-20.535 -34.984*	-20,075 -34.632*	-20,071 -34.703*
$\Delta S$ (kcal/mol.K)	-0.009 -0.012*	-0.009 -0.012*	-0,006 -0.013*	-0.007 -0.013*
$\Delta G$ (kcal/mol)	-17.946 -31.437*	-17.945 -31.437*	-18.174 -30.874*	-18.110 -30.951*

\* in 2-propanol solution

The results show the formation of four diastereoisomers P<sub>1</sub>, P<sub>2</sub>, P<sub>3</sub> and P<sub>4</sub> (Figure 1). The negative enthalpy in both the gas phase and in solution shows that the reaction is exothermic.

Values of enthalpy  $\Delta H$ , entropy  $\Delta S$  and Gibbs free energy  $\Delta G$  are all lower in solution, indicating that the thermodynamic aspect of the reaction is controlled by the solvent effect.

#### 4.4.2 Analysis of the potential energy surface and prediction of the reaction mechanism

Table 9 shows the energy values corresponding to the four diastereoisomers P<sub>1</sub>, P<sub>2</sub>, P<sub>3</sub> and P<sub>4</sub>, as well as those corresponding to the transition states TS<sub>1</sub>, TS<sub>2</sub>, TS<sub>3</sub>, TS<sub>4</sub>, TS<sub>1</sub><sup>#</sup>, TS<sub>2</sub><sup>#</sup>, TS<sub>3</sub><sup>#</sup>, TS<sub>4</sub><sup>#</sup> (E<sup>#</sup>), and the imaginary frequencies ( $f_i$ ) associated with these states in the gas phase and in solution. The table also shows the activation energy (E<sub>a</sub>) corresponding to the formation of each diastereoisomer, the transition energy differences as well as the product energy difference.

**Table 9:** Energies of reactants and products, transition state energy (E<sup>#</sup>), activation energy (E<sub>a</sub>) corresponding to the formation of the four diastereoisomers and imaginary frequencies ( $f_i$ ) associated with the four transition states in the gas phase and in 2-propanol solution calculated by DFT B3LYP/6-311G (d, p)

	TS <sub>1</sub> (path R, S)	TS <sub>2</sub> (path S, R)	TS <sub>3</sub> (path S, S)	TS <sub>4</sub> (path R, R)
$E_{products}$ (a.u.)	-6326.120 -6326.189*	-6326.120 -6326.189*	-6326.119 -6326.181*	-6326.119 -6326.181*
$E_{reactants}$ (a.u.)	-6325.990 -6326.036*			
$E^{\#}$ (a.u.)	-6325.908 -6325.972*	-6325.899 -6325.965*	-6325.909 -6325.970*	-6325.900 -6325.967*
$f_i$ (cm <sup>-1</sup> )	-240.620i -235.534i*	-237.228i -207.975i*	-365.628i -330.143i*	-374.990i -300.890i*
$E_a$ (kcal/mol)	51.456 40.161*	57.103 44.553*	50.828 41.416*	56.476 43.298*
$\Delta(E^{\#}_{TS_1} - E^{\#}_{TS_1^*})$ (kcal/mol)	11.29			
$\Delta(E^{\#}_{TS_3} - E^{\#}_{TS_3^*})$ (kcal/mol)	9.41			
$\Delta(E^{\#}_{TS_2} - E^{\#}_{TS_2^*})$ (kcal/mol)	12.55			
$\Delta(E^{\#}_{TS_4} - E^{\#}_{TS_4^*})$ (kcal/mol)	13.19			
$\Delta(E^{\#}_{TS_4^*} - E^{\#}_{TS_1^*})$ (kcal/mol)	3.14			
$\Delta(E_{P_3/P_4} - E_{P_1/P_2})$ (kcal/mol)	0.63 5.02*			

\* in 2-propanol solution

Notes to Table 9:

- i = imaginary frequency

The potential energy profile corresponding to the four diastereoisomers formed by the reaction between isopropyl dibromoacetate and isobutyraldehyde in the gas phase and in 2-propanol solution is shown in Figure 7.

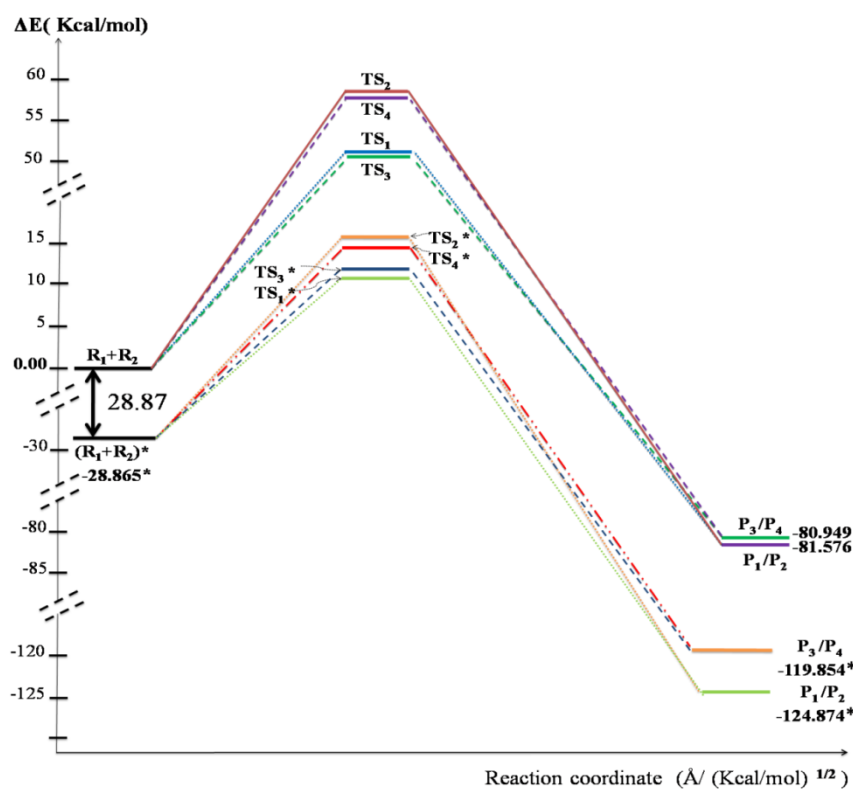


**Fig. 7:** Energy profile of the reaction between isopropyl dibromoacetate ( $R_2$ ) and isobutyraldehyde ( $R_1$ ) (kcal/mol)

Table 9 shows that:

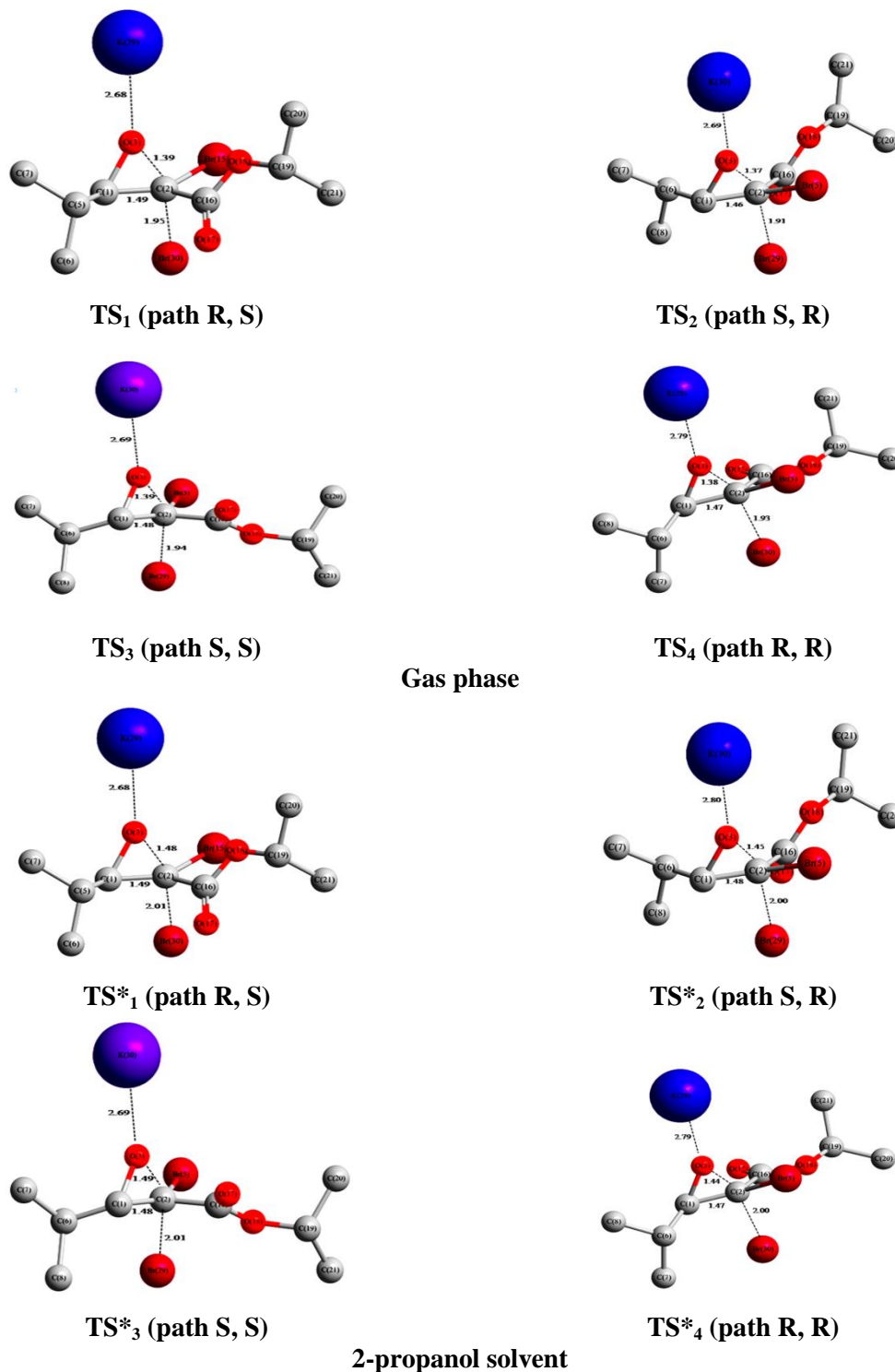
- The four transition states are characterized by a single imaginary frequency in the Hessian matrix;
- The activation energies corresponding to the forming of the four diastereoisomers  $P_1$  (1R, 2S),  $P_2$  (1S, 2R),  $P_3$  (1S, 2S) and  $P_4$  (1R, 2R) in solution are lower than those found in the gas phase [45], showing that the kinetic aspect of this reaction is facilitated by the solvent;
- The energy gap between transition states  $TS_2^*$  (path R, S) and  $TS_3^*$  (path S, S) is 3.19 kcal/mol and that between transition states  $TS_4^*$  (path R, R) and  $TS_1^*$  (path S, R) is 3.14 kcal/mol. This indicates that the two diastereoisomers  $P_1$  (1S, 2R) and  $P_3$  (1S, 2S) are kinetically preferred to the two diastereoisomers  $P_2$  (1R, 2S) and  $P_4$  (1R, 2R);
- The energy difference between the trans-diastereoisomers  $P_1/P_2$  and the cis-diastereoisomers  $P_3/P_4$  is 5.02 kcal/mol in 2-propanol solution and 0.63 kcal/mol in the gas phase, indicating that diastereoselectivity is dominated by the solvent effect.

Figure 5 shows that:

- The reactants and products are more stable in 2-propanol solution.
- The transition states of the four structures associated with the reaction paths (R, S), (S, R), (S, S) and (R, R) in 2-propanol solution are more stable than in the gas phase [54]. Furthermore, the structures associated with the reaction paths (R, S) and (S, S) are more stable than those associated with reaction paths (S, R) and (R, R).
- The two diastereoisomers ( $P_1$  (1R, 2S),  $P_2$  (1S, 2R)) and ( $P_3$  (1S, 2S),  $P_4$  (1R, 2R)) in the gas phase and in 2-propanol solution are isoenergetic.
- The four  $\alpha$ -brominated glycidic esters  $P_1$  (R, 2S),  $P_2$  (1S, 2R),  $P_3$  (1S, 2S) and  $P_4$  (1R, 2R) are more stable in solution than in the gas phase. Furthermore, the two trans-diastereoisomers are more stable than the cis form. This indicates that the thermodynamic aspect of this reaction is controlled by the solvent effect.

- The condensation of isopropyl dibromoacetate with isobutyraldehyde is diastereoselective, possibly because the groups attached to carbon atoms C<sub>(1)</sub> and C<sub>(2)</sub> of the epoxide ring have a steric effect.

In order to determine the interatomic distances involved in the condensation reaction between isopropyl dibromoacetate and isobutyraldehyde, we have presented in Figure 8 the four structures of the transition state of the four optimized diastereoisomers in the gas phase and dissolved in 2-propanol.



**Figure 8:** Structures of the transition states in the reaction between isopropyl dibromoacetate and isobutyraldehyde (distances in Å) determined using DFT B3LYP/ 6-311G (d, p)

The extent of the synchronicity  $\Delta d$  of bond-formation can be measured as the difference between the lengths of the two  $\sigma$  bonds formed in the transition state [46-47], that is,  $\Delta d = |d(C_{(1)}-C_{(2)}) - d(C_{(2)}-O_{(3)})|$ . The interatomic distances involved in the condensation reaction between isopropyl dibromoacetate and isobutyraldehyde in the gas phase and in solution as well as the difference  $\Delta d$  are given in Table 10.

**Table 10:** Interatomic distances of the transition states involved in the condensation reaction between isopropyl dibromoacetate and isobutyraldehyde (Å)

TS <sub>1</sub> (path R, S)		TS <sub>2</sub> (path S, R)		TS <sub>3</sub> (path S, S)		TS <sub>4</sub> (path R, R)	
C <sub>(1)</sub> -C <sub>(2)</sub>	1.49 1.49*	C <sub>(1)</sub> -C <sub>(2)</sub>	1.48 1.47*	C <sub>(1)</sub> -C <sub>(2)</sub>	1.48 1.48*	C <sub>(1)</sub> -C <sub>(2)</sub>	1.47 1.47*
C <sub>(2)</sub> -O <sub>(3)</sub>	1.48 1.39*	C <sub>(2)</sub> -O <sub>(3)</sub>	1.45 1.37*	C <sub>(2)</sub> -O <sub>(3)</sub>	1.49 1.39*	C <sub>(2)</sub> -O <sub>(3)</sub>	1.44 1.38*
C <sub>(2)</sub> -Br <sub>(30)</sub>	2.01 1.95*	C <sub>(2)</sub> -Br <sub>(29)</sub>	2.00 1.91*	C <sub>(2)</sub> -Br <sub>(29)</sub>	2.01 1.94*	C <sub>(2)</sub> -Br <sub>(30)</sub>	2.00 1.93*
O <sub>(3)</sub> -K <sub>(29)</sub>	2.68 2.68*	O <sub>(3)</sub> -K <sub>(30)</sub>	2.80 2.79*	O <sub>(3)</sub> -K <sub>(30)</sub>	2.69 2.69*	O <sub>(3)</sub> -K <sub>(29)</sub>	2.79 2.79*

\* in 2-propanol solution

Table 10 shows that the bond lengths C<sub>(2)</sub>-O<sub>(3)</sub> and C-Br are significantly affected by 2-propanol solution along the reaction pathway. However it does not substantially modify the bond lengths C<sub>(1)</sub>-C<sub>(2)</sub> and O-K.

We calculated IRC and in Figure 9 we plot the curves E=f(IRC) of the reaction pathway in solution.

Figure 7 shows that the four reaction paths have an early transition state both in the gas phase [45] and in solution. A transition state is called early if it is closer to the reactant side of the reaction coordinate than to the product side. According to Hammond's postulate [48], early transition states are a general characteristic of rapid exothermic reactions. This is also observed experimentally [1].

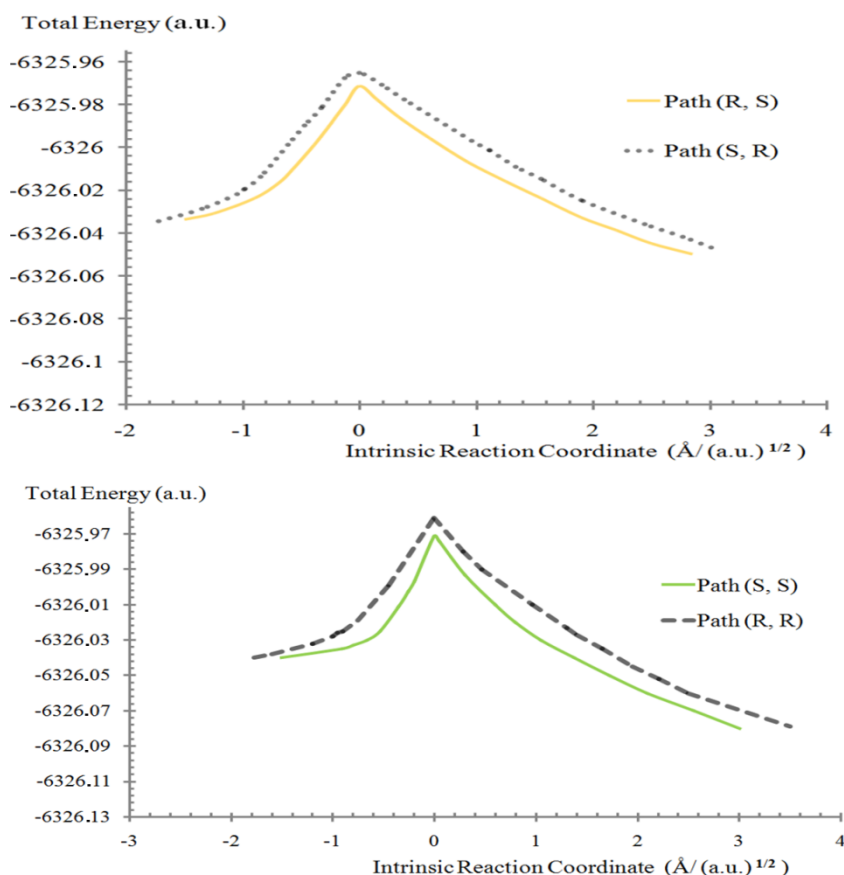


**Figure 9:** IRC of the reaction between isopropyl dibromoacetate and isobutyraldehyde calculated by B3LYP/6-311G (d, p) in 2-propanol solution

## Conclusion

The effect of the 2-propanol solvent on the reaction between isobutyraldehyde and isopropyl dibromoacetate was studied using DFT B3LYP/6-311G (d, p). Results showed that:

- Electron density of certain atoms of the reactants and isodensity maps of the LUMO of isobutyraldehyde and HOMO of isopropyl dibromoacetate are affected by the 2-propanol solvent.
- The interaction between the C<sub>(14)</sub> atom of isopropyl dibromoacetate and the C<sub>(1)</sub> atom of isobutyraldehyde is more favored in 2-propanol solution than in the gas phase.
- The electrophilic and nucleophilic character, local electrophilicity and local nucleophilicity, as well as atomic electronic populations and reactivity indices determined using NPA analysis are clearly modified by the solvent.
- The C<sub>(14)</sub>-C<sub>(1)</sub> attack is correctly predicted by the Fukui functions.
- The activation barrier corresponding to the four reaction paths is significantly lowered in solution and therefore the reaction between isopropyl dibromoacetate and isobutyraldehyde is accelerated.
- The kinetic reaction rates are affected by the solvent.
- The formation of the  $\sigma$  bonds C<sub>(1)</sub>-C<sub>(2)</sub> and C<sub>(2)</sub>-O<sub>(3)</sub> follows a synchronous process along the reaction pathway in the gas phase and in solution.
- The reaction between isobutyraldehyde and isopropyl dibromoacetate results in the formation of four diastereoisomers: P<sub>1</sub> (1R, 2S), P<sub>2</sub> (1S, 2R) of trans form and P<sub>3</sub> (1S, 2S), P<sub>4</sub> (1R, 2R) of cis form. Cis-isomers are not thermodynamically favored relative to trans-isomers, either in solution or in the gas phase. This result is in good agreement with the experimental results.
- The reaction pathway is exothermic in the gas phase as well as in solution.

The formation of  $\alpha$ -bromoglycidic esters has already been studied experimentally and the theoretical results we have obtained correspond well with the experimental data regarding the nature and proportion of products formed, both in the gas phase and in solution. Our results are also in agreement with experimental results as regards local and global reactivity, the exothermic nature of the reaction and the nature of the transition structures. However there is insufficient experimental data available regarding thermodynamic and kinetic values with which to compare with our results. We hope that the theoretical investigations presented in this modest work will be of value to further research.

## References

1. Legris C., *Thèse d'Etat, Paris VI* (1972) 60.
2. Coutrot P., Combret J. C., Villieras J., *Tetrahedron Lett.* 12 (1971) 1553-1556.
3. Coutrot P., Combret J. C., Villieras J., *CR. Hebd. Acad. Sci.* 270 (1970) 1674-1677.
4. Coutrot P., Legris C., *Synthesis* 2(1975) 118-120.
5. Coutrot P., El Gadi A., *J. Organomet. Chem.* 280 (1985) C11- C13.
6. Coutrot P., Grison C., Tabyaoui M., *Tetrahedron Lett.* 34(1993) 5089-5092.
7. Coutrot P., Dumarçay S., Finance C., Tabyaoui M., Tabyaoui B., Grison C., *Bioorg. Med. Chem. Lett.* 9 (1999) 949-952.
8. Becke A. D., *J. Chem. Phys.* 98(1993) 5648-5652.
9. Tomasi J., Persico M., *Chem. Rev.* 94(1994) 2027-2094.
10. Simkin B. Y., Sheikhet I., *Quantum Chemical and Statistical Theory of Solutions: A Computational Approach*, Ellis Horwood: London, UK. 1995.
11. Domingo L. R., Ríos-Gutiérrez M., Pérez P., *Tetrahedron* 71 (2015) 2421-2427.
12. Frisch M. J and al., *Gaussian 09* (2009) Gaussian Inc, Wallingford CT.
13. Dennington R., Keith T, Millam J., *GaussView, Version 5*, (2009).Semicem Inc., Shawnee Mission, KS.
14. Lee C., Yang W., Parr R. G., *Phys. Rev. B.* 37 (1988) 785-789.
15. Castro E. V. R. Jorge F. E., *J. Chem. Phys.* 108 (1998) 5225-5229.
16. Schlegel H. B., In *Modern Electronic Structure Theory*, ed. by Yarkony D. R., World Scientific Publishing: Singapore. (1995) 459-500.
17. Cancès M. T., Mennucci V., Tomasi J., *J. Chem. Phys.* 107 (1997) 3032-3041.

18. Cossi M., Barone V., Cammi R., Tomasi J., *J. Chem. Phys. Lett.* 255 (1996) 327-335.
19. Barone V., Cossi M., Tomasi J., *J. Comput. Chem.* 19 (1998) 404-417.
20. Domingo L. R., Arno M., Contreras R., Pérez P., *J. Phys. Chem. A* 106 (2002) 952-961.
21. Parr R. G., Donnelly R. A., Levy M., Palke W. E., *J. Chem. Phys.* 68 (1978) 3801-3807.
22. Domingo L. R., Aurell M. J., Pérez P., Contreras R., *Tetrahedron* 58 (2002) 4417-4423.
23. Parr R. G., Yang W., *J. Am. Chem. Soc.* 106 (1984) 4049-4050.
24. Yang W. T., Mortier W. J., *J. Am. Chem. Soc.* 108 (1986) 5708-5711.
25. Domingo L. R., Aurell M. J., Pérez P., Contreras R., *J. Phys. Chem. A* 106 (2002) 6871-6875.
26. Pérez P., Domingo L. R., Aurell A. J., Contreras R., *Tetrahedron* 59 (2003) 3117-3125.
27. Pérez P., Domingo L. R., Aizman A., Contreras R., In *Theoretical Aspects of Chemical Reactivity*, Vol. 19, ed. by Toro-Labbé, A., Elsevier Science: Amsterdam. 19 (2007) 139-201.
28. Pérez P., Domingo L. R., Duque-Noreña M., Chamorro E. A., *J. Mol. Struct. Theochem* 895 (2009) 86-91.
29. Domingo L. R., Pérez P., Sàez J. A., *RSC Advances* 3 (2013) 1486-1494.
30. Kohn W., Sham L., *Phys. Rev.* 140 (1965) 1133-1138.
31. Domingo L. R., Chamorro E. A., Pérez P., *J. Org. Chem.* 73 (2008) 4615-4624.
32. Geerlings P., De Proft F., Langenaeker W., *Chem. Rev.* 103 (2003) 1793-1873.
33. Pearson R. G., *J. Chem. Ed.* 64 (1987) 562.
34. Pearson R. G., Palke W. E., *J. Phys. Chem.* 96 (1992) 3283.
35. Parr R. G., Chattaraj P. K., *J. Am. Chem. Soc.* 113 (1991) 1854.
36. Chattaraj P. K., Sengupta S. J., *J. Phys. Chem.* 103 (1999) 6122.
37. Domingo L. R., Pérez P., *Org. Biomol. Chem.* 9 (2011) 7168-7175.
38. Mebi C. A., *J. Chem. Sci.* 123 (2011) 727-731.
39. Chemouri H., Mekelleche S. M., *J. Mol. Struct. THEOCHEM* 813 (2007) 67-72.
40. Chattaraj P. K., Giri S., *Annu. Rep. Prog. Chem. C* 105 (2009) 13-39.
41. Chattaraj P. K., Sarkar U., Roy D. R., *Chem. Rev.* 106 (2006) 2065-2091.
42. Gazquez J. L., Mendez F., *J. Phys. Chem.* 98 (1994), 4591-4593.
43. Houk K. N., *Acc. Chem. Res.* 8 (1975) 361-369.
44. Reed A. E., Weinstock R. B., Weinhold F., *J. Chem. Phys.* 83 (1985) 735-746.
45. Lakbaibi Z., Abou El Makarim H., Tabyaoui M., El Hajbi A., *Moroccan J. Chem.*, 3, (2016) 432-453
46. Rhyman L., Ramasami P., Joule J. A., Domingo L. R., *Comp. Theor. Chem.* 1025 (2013) 58-66.
47. Karbalaei Khani S., Cundari T. R., *Comp. Theor. Chem.* 1056 (2015) 61-73.
48. Hammond G. S., *J. Am. Chem. Soc.*, 77 (1955) 334-338.

(2016) ; <http://www.jmaterenvirosci.com/>